J Fluoresc (2014) 24:169–181
DOI 10.1007/s10895-013-1283-x

ORIGINAL PAPER

Synthesis, Characterization, DNA Binding Studies, Photocleavage, Cytotoxicity and Docking Studies of Ruthenium(II) Light Switch Complexes

Nazar Mohammed Gabra · Bakheit Mustafa · Yata Praveen Kumar · C. Shobha Devi · A. Srishailam · P. Venkat Reddy · Kotha Laxma Reddy · S. Satyanarayana

Received: 7 March 2013 / Accepted: 9 August 2013 / Published online: 28 August 2013

Abstract A new ligand 3-(1*H*-imidazo[4,5-*f*][1,10] phenanthrolin-2yl)phenylboronic acid and its (IPPBA) three ruthenium(II) complexes $[Ru(phen)_2(IPPBA)](ClO_4)_2$ (1), $[Ru(bpy)_2(IPPBA)](ClO_4)_2$ (2) and $[Ru(dmb)_2(IPPBA)](ClO_4)_2$ (3) have been synthesized and characterized by elemental analysis, UV/VIS, IR, ^{1}H-NMR,^{13}C-NMR and mass spectra. The binding behaviors of the three complexes to calf thymus DNA were investigated by absorption spectra, emission spectroscopy, viscosity measurements, thermal denaturation and photoactivated cleavage. The DNA-binding constants for complexes 1, 2 and 3 have been determined to be 7.9×10^5 M^{-1}, 6.7×10^5 M^{-1} and 2.9×10^5 M^{-1}. The results suggest that these complexes bound to double-stranded DNA in an intercalation mode. Upon irradiation at 365 nm, three ruthenium complexes were found to promote the cleavage of plasmid pBR322 DNA from super coiled form I to nicked form II. Further in the presence of Co^{2+}, the emission of DNA–Ru(II) complexes can be quenched. And when EDTA was added, the emission was recovered. The experimental results show that all three complexes exhibited the "on–off–on" properties of molecular "light switch". The highest Cytotoxicity potential of the complex1 was observed on the Human alveolar adenocarcinoma (A549) cell line. Good agreement was generally found between the spectroscopic techniques and molecular docked model which provides further evidence of groove binding.

Keywords Polypyridyl Ru(II) complexes · DNA-binding · Molecular light switch · Molecular docking · Photocleavage

N. M. Gabra · B. Mustafa · Y. P. Kumar · C. S. Devi · A. Srishailam · P. V. Reddy · K. L. Reddy · S. Satyanarayana (✉)
Department of Chemistry, Osmania University, Hyderabad, Andhra Pradesh PIN-500007, India
e-mail: ssnsirasani@gmail.com

N. M. Gabra
Department of Chemistry, Red Sea University, Portsudan P.O. Box: 24, Sudan

Introduction

The design and development of new anticancer drugs is an active area of research in chemical science. After the discovery of cisplatin by Rosenberg [1] as an effective anticancer drug having various side effects, the search for alternative metal based drugs has been an important area of interest for researchers. Among the several metals that are currently being investigated for their anticancer activity, ruthenium occupies a prominent position. Due to their rich photochemistry polypyridyl complexes of ruthenium(II)-have received considerable attention as DNA binding substrates. They are photochemical stable in their ground and excited state, and have long lived triplet states, rich redox/spectral properties and good water solubility [2]. Furthermore, judicious selection of coordinated ligands can be used to tune the photochemistry and DNA binding properties of these systems. The rich optical properties of these complexes also facilitate assessments of their DNA binding capabilities as binding to DNA can be probed through changes in absorption and emission spectra.

Polypyridyl transitional metal complexes can bind to DNA by non-covalent interactions such as external surface binding for cations, groove binding for large molecules and intercalation for planar molecules or compounds containing a ring

system. Among the factors governing the binding modes, it appears that the most significant is the molecular shape. Those complexes that best fit against the DNA helical structure display the highest binding affinity [3]. Many useful applications of these complexes require that the complex bind to DNA through an intercalative mode with the ligand intercalating into the adjacent base pairs of DNA. By changing the metal ions the geometry of the complex (square planar, tetrahedral, octahedral, etc.) may be modified and consequently its photophysical properties, and may affect its interaction with nucleic acids. By varying the ligands, it is possible to modify the mode of interaction of the complex with nucleic acids [4–8]. In fact, some of these complexes also exhibit interesting properties upon binding to DNA [9–12]. In this paper, we synthesized three complexes of Ru(II) 3-(1*H*-imidazo[4,5-*f*][1,10]phenanthrolin-2yl)phenylboronic acid, and studied their binding properties to calf thymus DNA using absorption spectroscopy, fluorescence spectroscopy, viscosity measurements and molecular docking analysis of Ru(II) complexes to duplex DNA of sequence (GCTGCAAAC GTCG/CGACGNTGCAGC) (PDB ID: 2L8I). Their photocleavage behavior toward pBR 322. Recently Sun Dongdong et al. [13] studied the effects of luminescent ruthenium(II) polypyridyl (phenyl boronic acid) functionalized selenium nanoparticles on bFGF-induced angiogenesis and AKT/ERK signaling. The results should be of value in understanding the binding mode of the complex to DNA, as well as laying the foundation for the rational design of a DNA molecular light switch and DNA cleaving agents [14].

Experimental

Chemicals

All reagents and solvents were purchased commercially and used without further purification unless otherwise noted. $RuCl_3$, 1,10-Phenanthroline monohydrate and pyridines were purchased from Merck, calf thymus (CT) DNA was purchased from Aldrich and supercoiled pBR 322 DNA was obtained from Fermentas life sciences. All experiments involving the interaction of the complexes with DNA were carried out in double distilled buffer (5 mM Tris–HCl, 50 mM NaCl, pH 7.2). A solution of calf thymus DNA in the buffer gave a ratio of UV absorbance at 260 and 280 nm of about 1.8–1.9:1, indicating that the DNA was sufficiently free of protein [15]. The DNA concentration per nucleotide was determined by absorption spectroscopy using the molar absorption coefficient 6600 M^{-1} cm^{-1} at 260 nm [16].

Synthesis of Ligand and Complexes

1,10-Phenanthroline-5,6-dione [17], 1H-imidazo[4,5-f][1,10]phenanthrolin-2yl) phenylboronic acid [18] and $[Ru(L)_2Cl_2]^{2+}$ [19] was synthesized by the reported procedure. Figure 1 shows Synthetic scheme of the complexes

Synthesis of $[Ru(phen)_2IPPBA](ClO_4)_2 . 2H_2O$ (1)

A mixture of cis-$[Ru(phen)_2(Cl)_2] \cdot 2H_2O$ (0.10 g,0.16 mM) and (IPPBA) (0.054 g,0.16 mM) in ethanol (30 mL) was

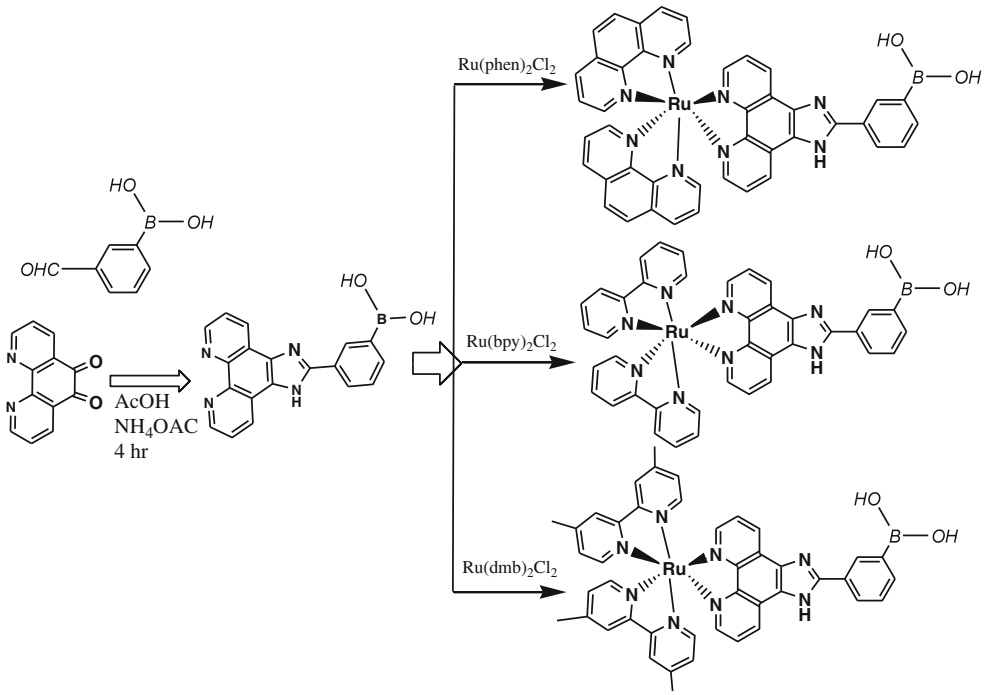

Fig. 1 Synthesis and structure of the Ru(II)complexes

refluxed under nitrogen for 8 h to give a clear red solution . Upon cooling, a red precipitate was obtained by dropwise addition of saturated aqueous $NaClO_4$ solution. The solid was collected washed with small amounts of water, ethanol, and diethyl ether, then dried under vacuum, Yield (72 %), Analytical data for Ru $C_{43}H_{33}BN_8Cl_2O_{12}$, Calcd (%) C: 64.43; H: 3.65; N: 13.98 found: C: 65.13, H: 3.91, N: 14.22 LCMS in DMSO M/Z: 1031.

Synthesis of $[Ru(bpy)_2IPPBA](ClO_4)_2.2H_2O$ (2)

This complex was synthesized as described above complex (1).yield (69 %). Analytical data for $RuC_{39}H_{33}BN_8Cl_2O_{12}$: Calcd: C: 62.16; H: 3.88; N: 14.87; found C:62.51; H :4.10; N : 14.90; LCMS in DMSO M/Z: 1040. Figures 2 and 3 shows ^1H and ^{13}C NMR spectrum of $[Ru(bpy)_2IPPBA]^{2+}$

Synthesis of $[Ru(dmb)_2IPPBA](ClO_4)_2.2H_2O$ (3)

This complex was synthesized as described above complex (1).yield (69 %). Analytical data for RuC_{39} $H_{33}B$ $N_8C_{l2}O_{12}$: Calcd: C: 62.16; H: 3.88; N: 14.87; found C:62.51; H :4.10; N : 14.90; LCMS in DMSO M/Z: 1040. found:1042 For all the complexes IR, ^1H- ^{13} C [^1H]-NMR, data are given in (Tables 1 and 2).

Physical Measurements

Microanalyses (C, H and N) were carried out with Perkin-Elmer 240 elemental analyser. UV–vis spectra were recorded on an Elico Bio-spectrophotometer model BL198, Emission spectra recorded with Elico Bio-spectro fluorimeter model S L 174. and NMR spectra was recorded on Bruker 400 MHz spectrometer with DMSO-d_6 as a solvent at room temperature and TMS as the internal standard. IR spectra were obtained in KBr phase on a Perkin–Elmer FTIR 1605. NMR spectra were measured with Bruker 400 MHz spectrometer with DMSO-d_6 as a solvent at room temperature and TMS as the internal standard. LC-MS 2010 A Shimadzu Japan.. Viscosity experiments were carried on Ostwald viscometer, immersed in thermostatted water-bath maintained at 30±0.1 °C. CT-DNA samples approximately 200 base pairs in average length were prepared by sonication in order to minimize complexities arising from DNA flexibility [20]. Data were presented as $(\eta/\eta^0)^{1/3}$ versus binding ratio [21], where η is the viscosity of CT-DNA in the presence of complex, and η^o is the viscosity of CT-DNA alone. Viscosity values were calculated from the observed flow time of DNA-containing solutions ($t > 100\ s$) corrected for that of buffer alone (t_0),$\eta=(t'- t_0)/t_0$.

For the gel electrophoresis experiments, supercoiled pBR 322 DNA (0.1 mg) was treated with Co(III) complexes in 50 mM Tris–acetate, 18 mM NaCl buffer, pH 7.2, and the solutions were then irradiated at room temperature with a UV lamp (302 nm, 10 W). The samples were analyzed by electrophoresis for 3 h at 25 V on a 1 % agarose gel in Tris–acetate buffer. The gel was stained with ethidium bromide and photographed under UV light.

In Vitro Cytotoxicity Assay

Human cervical cancer cells, A549 (ATCC No. CCL-185) derived from human alveolar adenocarcinoma epithelial cells,

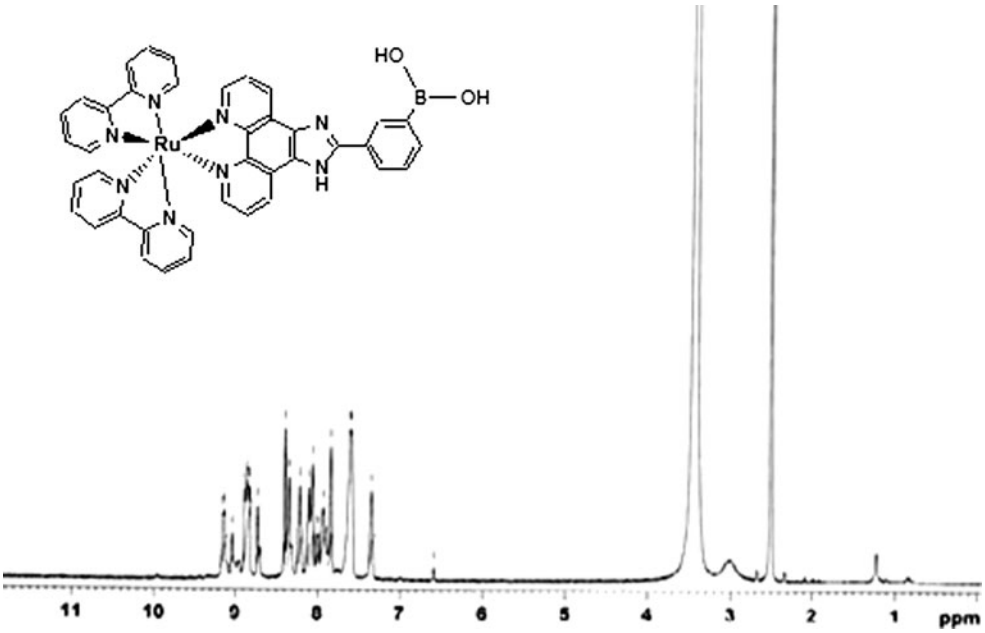

Fig. 2 The ^1H-NMR (DMSO-d_6, TMS, δ-ppm) spectrum of $[Ru(bpy)_2IPPBA]^{2+}$

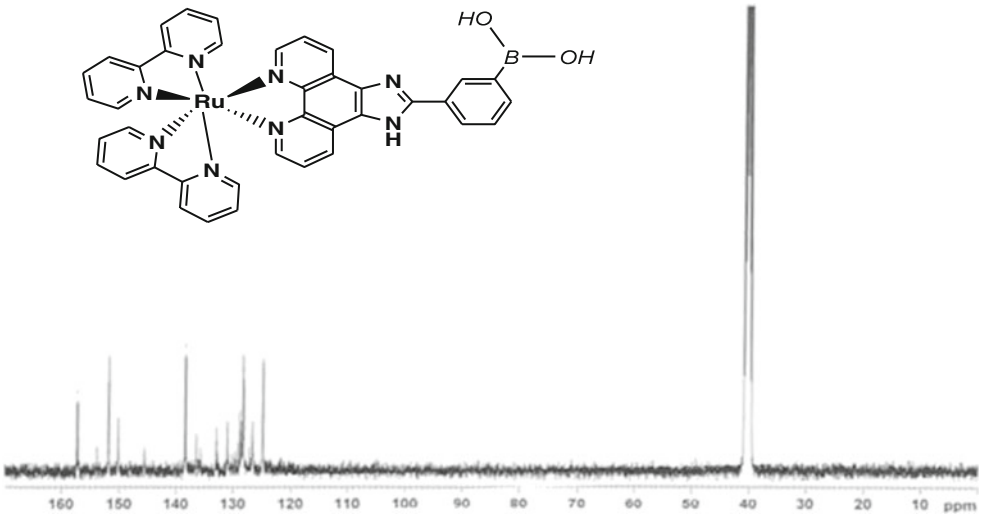

Fig. 3 The $^{13}C[^{1}H]$-NMR (DMSO-d_6, δ-ppm) spectrum of $[Ru(bpy)_2IPPBA]^{2+}$

MDA-MB-231 (ATCC No. HTB-26) and MCF7 (ATCC No. HTB-22) derived from human breast adenocarcinoma cells were maintained in cell-mediated reduction of tetrazolium salt to form water insoluble formazan crystals using the standard MTT (3-{4,5-dimethylthiazol-2-yl}-2,5-diphenyltetrazolium bromide) cellular viability assay [13, 22] using doxorubicin as positive control. The cells were left for 48 h to rest, and afterwards investigated agents were added. Preparation of tested solution was performed immediately before experiment, by dissolution in DMSO to the stock concentration of 10 mM, whereas further dilutions were used. Dose–response curves were plotted for the test compounds and controls after correction by subtracting the background absorbance from that of the blanks. Results are finally expressed as IC50 values (concentration of investigated agent that declines the number of viable cells by 50 % in treated cell population compared to untreated control).

Docking Studies

All dockings were performed as blind dockings using Gold 3.0.1 (Genetic Optimization for Ligand Docking) program [23, 24] which is based on Genetic Algorithms. This method allows partial flexibility of the hydroxyl groups of the respective DNA molecule and full flexibility of the ligand, other parameters were default values. The Protein Data Bank was used to download the nucleic acid receptor (PDB ID: 2L8I) DNA duplex of sequence (GCTGCAAACGTCG/CGACGNTGCAGC). In order to evaluate the GOLD scoring function, all water molecules were removed from the DNA molecules. The function fitted was Gold Score:

$$\text{Fitness} = S(\text{hb–ext}) + 1.3750 \times S(\text{vdw–ext}) + \text{Sint}$$

where S(hb- ext) is the DNA-ligand hydrogen bond score, S(vdw- ext) is the DNA-ligand van der Waals score, Sint is the score from intramolecular ligand interactions [25].

DNA-Binding Experiments

Absorption Spectroscopic Studies

Due to the strong stacking interaction between aromatic chromophore of the complex and the base pairs of DNA, complex bound to DNA through intercalation usually results in hypochromism and red shift (bathochromism). Figure 4 shows the absorption spectra of $[Ru(phen)_2(IPPBA)](ClO_4)_2$ (1), $[Ru(bpy)_2(IPPBA)](ClO_4)_2$ (2) and $[Ru(dmb)_2(IPPBA)](ClO_4)_2$ (3) in the presence of increasing concentration of DNA. In the UV region, the intense absorption band observed in these complexes are attributed to intraligand π–π* transition. The low energy absorption band centered at 420–450 nm is assigned to metal-to-ligand charge transfer (MLCT) transition. As increasing the concentration of CT-DNA, the MLCT transition band of complexes 1,2 and 3 at 448, 445 nm and 442 nm exhibit hypochromism of 16.1, 15.2 and 10.6 %, and bathochromism of 9.2, 7.9 and 6.1 nm, respectively. However, the high hyperchromism effects observed suggest that van der Waals contacts between the OH group of the complex and the cytosine (in DNA) are also very important.

Based on the observations of complexes, we presume that there are some interactions between complexes and DNA. In order to further elucidate the binding strength of the complexes, the intrinsic constants K_b were determined by monitoring the changes of absorbance in the MLCT band with increasing concentration of CT-DNA. The intrinsic binding constant K_b for the interaction of the studied complexes with

Table 1 ^{1}H NMR and IR data of complexes

Complex	IR data(cm^{-1})				^{1}H-NMR (400 MHz, ppm DMSO-d6, TMS
	C = C	C = N	M-N(phen/bpy/dmp)	M-L	
$[Ru(phen)_2(IPPBA)]^{2+}$	1427	1606	623	721	9.10 (d, 2H, Ha, Ha′), 9.03 (d, 4H, H1, H1′), 8.78 (d, 4H, H3, H3′,), 8.76 (d, 2H, Hc, Hc′), 8.39 (s, 1H, Hm), 8.15(t, 4H, H6, H6′), 8.08(d, 2H, Ho, Hk), 8.00 (d, 2H, Hb, Hb′), 7.95 (d, 4H, H2, H2′), 7.40 (d, 1H, Hm), 2.50(2H, Hp, Hq)
$[Ru(bpy)_2(IPPBA)]^{2+}$	1445	1603	625	766	9.22 (d, 2H, Ha, Ha′), 9.07 (d, 4H, H1, H1′), 8.95 (d, 2H, Hc, Hc′), 8.70 (t, 4H, H3, H3′), 8.30 (d, 2H, Ho, Hk), 8.18 (t, 2H, 2H, Hb, Hb′), 7.98 (d,1H, Hn), 7.90 (d, 1H, Hm), 7.70 (t, 4H, H2, H2′), 2.60 (2H, Hp, Hq)
$[Ru(dmb)_2(IPPBA)]^{2+}$	1445	1603	626	765	9.03 (d, 2H, Ha, a′), 8.98 (d, 4H, H1,H1′), 8.73 (d, 4H, H4, H4′), 8.39 (d, 2H, Hc, Hc′), 7.90 (d, 2H, Ho, Hk), 7.85 (d, 1H, Hn), 7.60(t, 2H, 2H, Hb, Hb′),7.41 (d, 1H, Hm), 7.16 (t, 4H, H2, H2′), 2.60 (2H, Hp, Hq), 2.45 (12H, H6, H6′)

CT-DNA was calculated by absorption spectral titration data using the following equation

$$[DNA]/(\Sigma_a-\Sigma_f) = [DNA]/(\Sigma_b-\Sigma_f) + 1/K_b(\Sigma_b-\Sigma_f)$$

where [DNA] is the concentration of CT-DNA in base pairs, the apparent absorption coefficients ε_a, ε_f and ε_b correspond to A_{obsed}/[Ru], the absorbance for the free ruthenium complex, and the absorbance for the ruthenium complex in fully bound form, respectively. In plots of [DNA]//(ε_a-ε_f) versus [DNA],K_b is given by the ratio of slope to the intercept. Intrinsic binding constants, Kb of complexes 1, 2 and 3 are 7.9×10^5 M^{-1}, 6.7×10^5 $M^{-1}$and 2.9×10^5 M^{-1} . These Kb values are smaller than those of classical intercalators, such as $[Ru(bpy)_2(dppz)]^{2+}$ ($K=1.6\times10^6$) [4] and $[Ru(bpy)^2(ppd)]^{2+}$, ($K=1.3\times10^6$) [26] and much stronger than those of their parent complexes, $[Ru(bpy)_3]^{2+}$ (4.7×10^3 M^{-1}) and $[Ru(phen)_3]^{2+}$ (5.5×10^3 M^{-1}), [27] which can be explained as : (1) PIP possesses a larger planar area and extended π system than parent complexes, which leads to interact more deeply and makes stacking more strongly [28], (2) the intercalated ligand, IPPBA, contains two free hydroxy groups, which may form intermolecular hydrogen bonds with the base pairs. This factor is advantageous for the binding of complexes 1, 2 and 3 with DNA. These results also indicate that the size and shape of the intercalated ligand has a significant effect on the strength of DNA binding and the most suitable intercalating ligand leads to the highest affinity of the complexes for DNA. Additionally, from these results, we could deduce that both 1 and 2 bind to DNA by intercalation and their different DNA binding properties may be due to the ancillary ligands. Comparing phen and bpy, it is clear that the hydrophobicity and the surface area decrease in bpy, resulting in a weaker DNA binding affinity for complex 2.

Table 2 ^{13}C [^{1}H] NMR data of ligand and complexes

Complex	^{13}C NMR (100 MHz, ppm, DMSO-d6, major peaks)
$[Ru(phen)_2(IPPBA)]^{2+}$	153.82, 153.00, 151.90, 150.64, 147.87, 146.02, 143.43, 137.29, 136.38, 135.72, 132.93, 131.00, 126.48, 123.80.
$[Ru(bpy)_2(IPPBA)]^{2+}$	157.5, 157.3, 152.50, 152.06, 138.52, 138.24, 137.23, 128.50, 128.00, 127.07, 126.00, 125.01, 124.89, 124.81, 123.57, 122.85, 121.02.
$[Ru(dmb)_2(IPPBA)]^{2+}$	156.92, 154.30, 151.22, 150.00, 144.11, 135.56, 132.67, 130.09, 129.79, 128.80, 128.41, 125.20, 124.89, 123.61, 123.30, 121.80, 21.20.

Fluorescence Quenching and Competitive Binding

In the absence of DNA, complexes can emit luminescence in Tris buffer with emission maximum appearing at 598 nm. Upon addition of CT DNA the emission intensities of the complexes increase when compared to the intensity of complexes alone shown in Fig. 5. This implies that complexes can strongly interact with DNA and be protected by DNA efficiently, since the hydrophobic environment inside the DNA helix reduces the accessibility of solvent water molecules to the duplex and the complexes mobility is restricted at the binding site, lead to decrease in the vibrational modes of relaxation. This observation is further supported by the fluorescence quenching experiments using $[Fe(CN)_6]^{4-}$ as quencher to distinguish differentially bound Ru(II) species and positively charged free complex ions which should be readily quenched by $[Fe(CN)_6]^{4-}$. The complexes bound to DNA can be protected from the quencher, because highly negatively charged $[Fe(CN)_6]^{4-}$ would be repelled by the negative DNA phosphate backbone, hindering quenching of the emission of

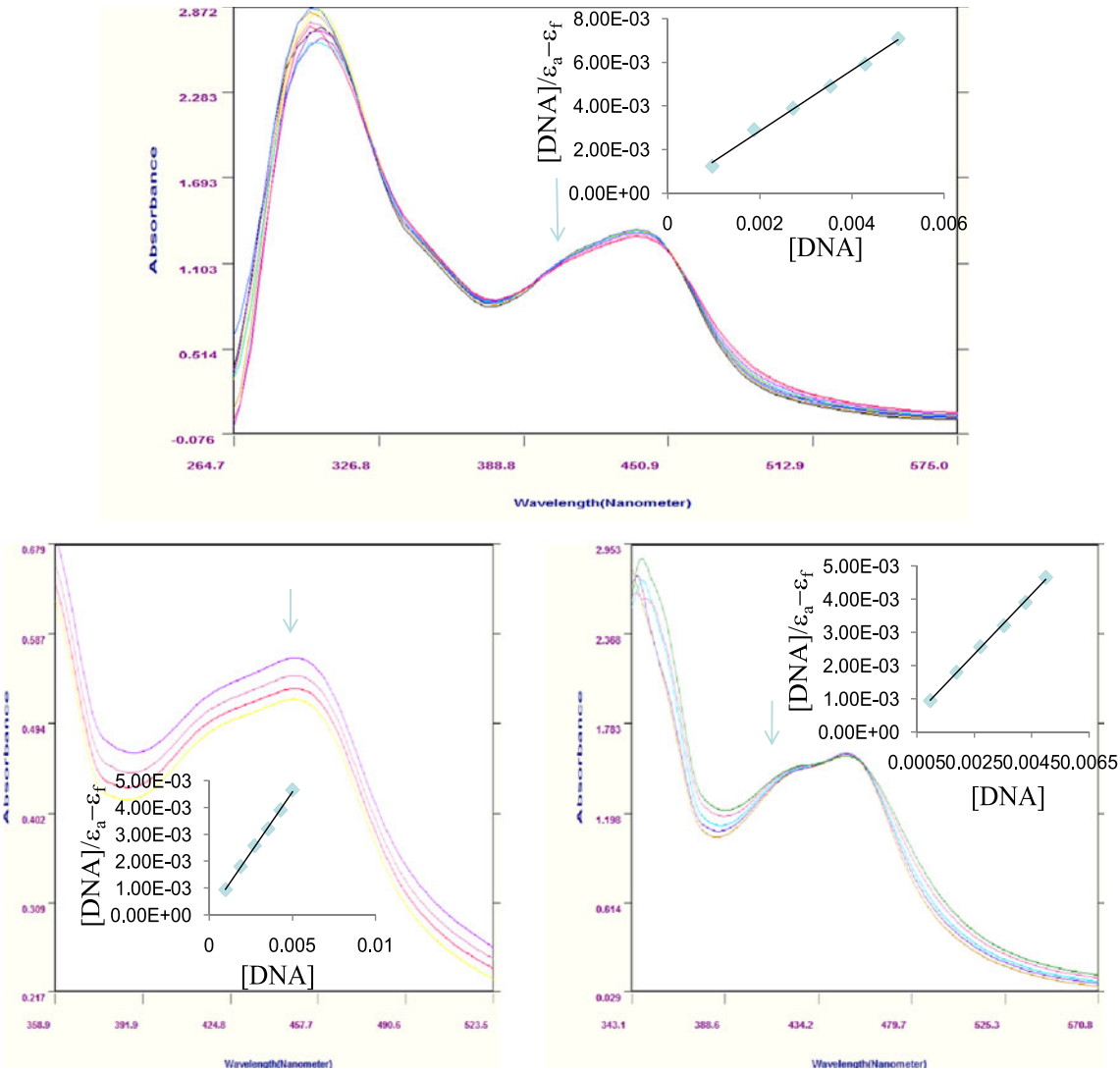

Fig. 4 Absorption spectra of $[Ru(phen)_2(IPPBA)](ClO_4)_2$ (1), $[Ru(bpy)_2(IPPBA)](ClO_4)_2$ (2) and $[Ru(dmb)_2(IPPBA)](ClO_4)_2$ (3) in Tris–HCl buffer upon addition of CT-DNA at room temperature in the presence of [complex]=20 μM. *Arrow* shows the absorbance changes upon increasing DNA concentrations. Insert plots of [DNA]/(Σa–Σf) *vs* [DNA] for the titration of Ru(II) complex

the bound complex. The method essentially consists of titrating a given amount of DNA-metal complexes with increasing the concentration of $[Fe(CN)_6]^{4-}$ and measuring the change in fluorescence intensity Fig. 6. Steady-state fluorescence quenching experiments with $[Fe(CN)_6]^{4-}$ as quencher can provide some information about binding of ruthenium(II) complexes with CT-DNA. The Stern–Volmer quenching constant (K_{sv}) can be determined by using Stern–Volmer equation [29]

$$I_0/I = 1 + K_{sv}[Q]$$

Where I_0 and I are the intensities of the fluorophore in the absence and presence of the quencher, respectively, Q is the concentration of the quencher and K_{sv} is a linear Stern–Volmer quenching constant. Figure 5 shows the Stern–Volmer plots for the free complex in solution and in the presence of increasing amounts of DNA. Highly negatively charged quencher is expected to be repelled by the negatively charged phosphate backbone, and therefore a DNA bound cationic complex should be less quenched by anionic quencher, than the unbound complex [30, 31]. All the complexes show linear Stern–Volmer plots. The K_{sv} values for the complexes in the absence of DNA are 225, 201 and 186 M^{-1} for 1, 2 and 3, respectively, while the K_{sv} values in the presence of DNA are 49, 38 and 22, respectively. Hence, for all three complexes in the presence of DNA, Ksv is smaller, and at a high concentration of DNA (1:200; Ru^{2+}: DNA), the plots have essentially zero slope, indicating that the bound species is inaccessible to the quencher. From the quenching studies also it is clear that DNA binding ability of complex follow the order 1>2>3.

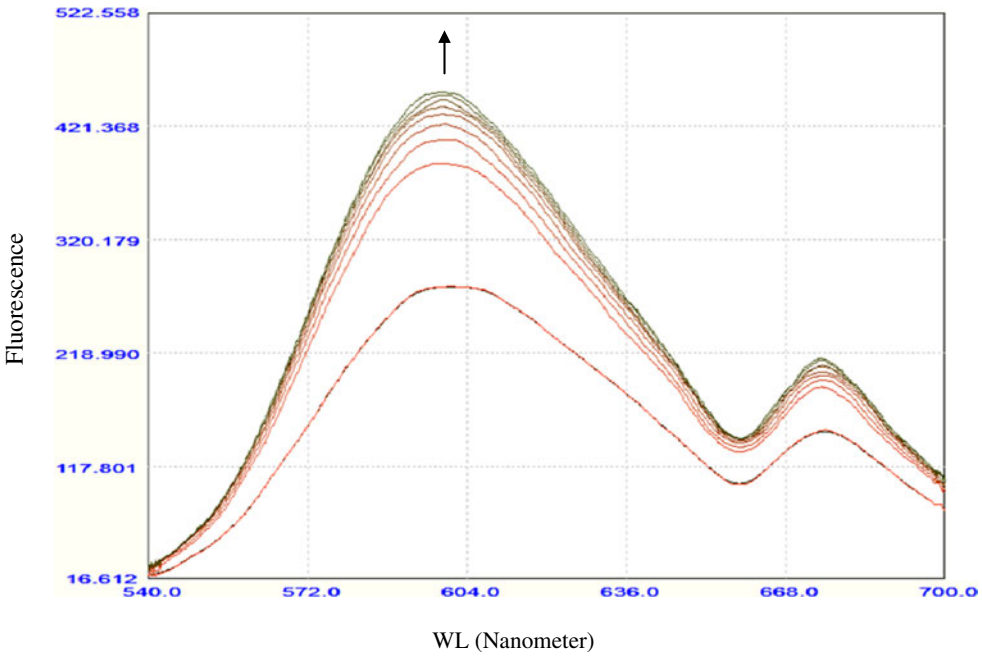

Fig. 5 Emission spectra of complex1in Tris–HCl buffer in the presence and absence of CT DNA, the emission intensity increase upon addition of CT DNA (0.5 μl, 10 μl, 15 μl—of DNA). *Arrow* shows the intensity change upon increasing DNA concentrations. Insert: plots of relative integrated emission intensity versus [DNA]/[Ru]

Light Switch Effect

The most interesting property of Ru(II) complexes are DNA molecular "light switches," which show no photoluminescence in aqueous solution but display intense photoluminescence in the presence of double helical DNA. The study of the molecular "light switch" was mainly about searching for a novel "light switch" and then investigating the interaction mode between the "light switch" complex and DNA. The emission of DNA-intercalated $[Ru(bpy)_2IPPBA]^{2+}$ (switch on) can be quenched

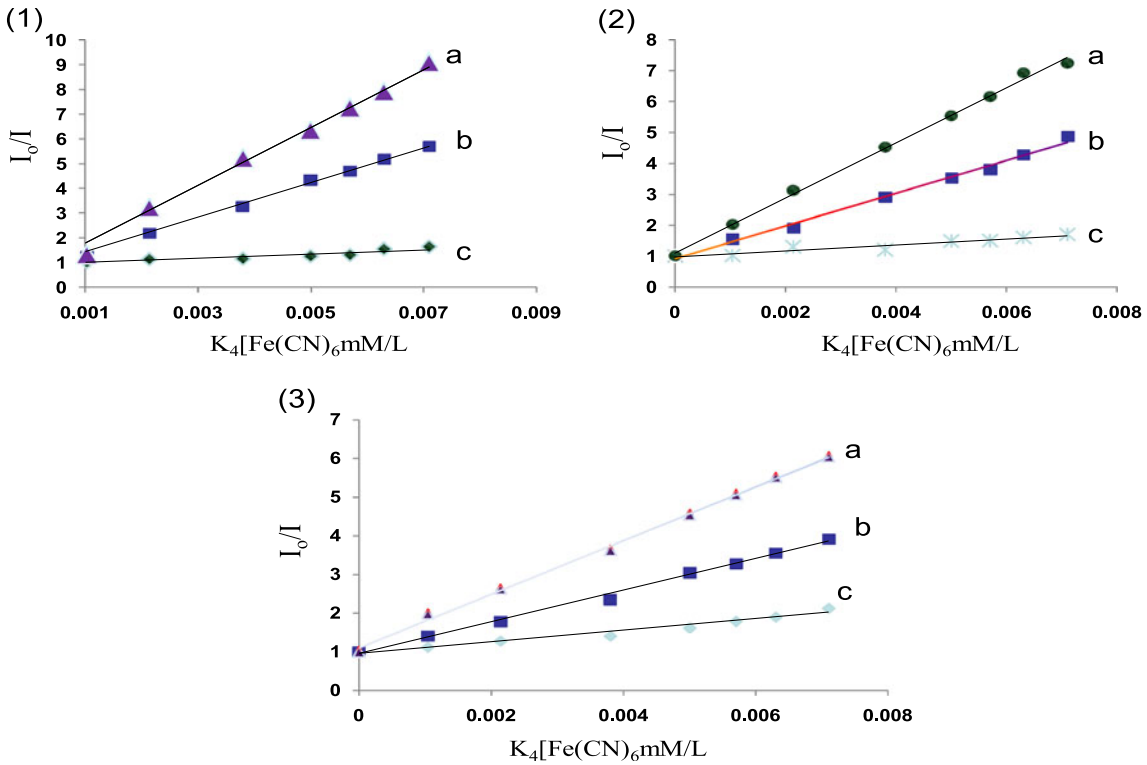

Fig. 6 Emission quenching of [$[Ru(phen)_2(IPPBA)]$ (1), $[Ru(bpy)_2(IPPBA)]$ (2) and $[Ru(dmb)_2(IPPBA)]$ (3) with $K_4[Fe(CN)_6]$ in the absence (**a**) and presence (**b**) [Ru]=20 μm, and excess of DNA (**c**)

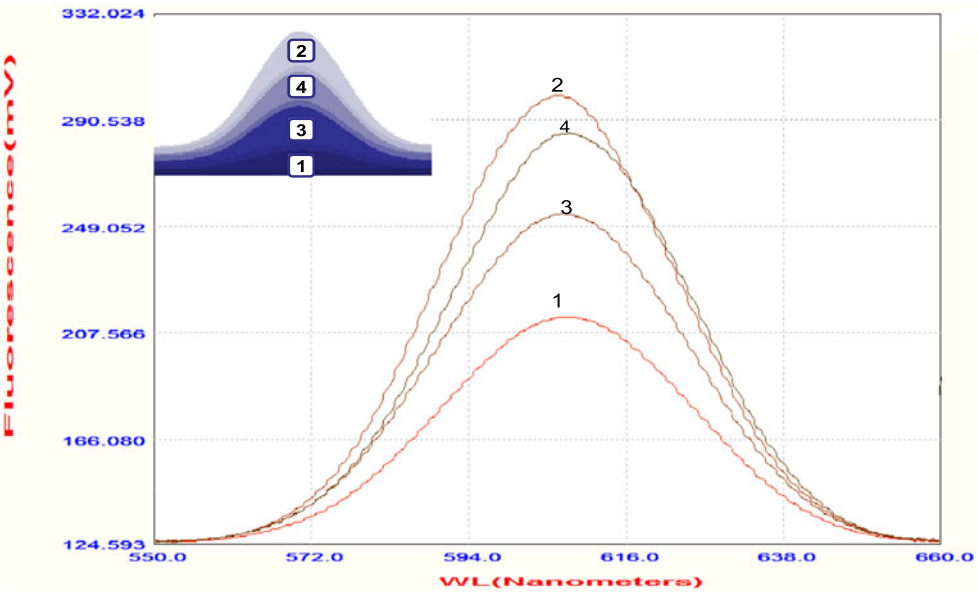

Fig. 7 $[Ru(pby)_2IPPBA]^{2+}$ in tris buffer(1), complex+DNA (2)(switch on), complex+DNA+ Co^{2+} (3)(switch off), and complex+DNA+Co^{2+} EDTA(4)

by various transition metal ions, thus turning the light switch off. The addition of Co^{2+} to complex bound to DNA quenches its fluorescence. The addition of an equimolar concentration of 5μM Co^{2+} to 5μM $[Ru(bpy)_2IPPBA]^{2+}$ bound to 200μM DNA (5 mM Tris, pH 7.5, 50 mM NaCl) results in the loss of almost 94 % of the luminescence due to the formation of Co^{2+}-$[Ru(bpy)_2IPPBA]^{2+}$ heterometallic complex.. It should be noted that the concentrations of Co^{2+} ions and EDTA required to turn the emission off and on are not equimolar due to the different binding constants of Co^{2+} for IPPBA and EDTA. Figure 7 shows the changes in the relative emission intensity of $[Ru(bpy)_2IPPBA]^{2+}$ bound to DNA as Co^{2+} and EDTA are added successively, thus flipping the DNA light switch on and off over a series of cycles. In this system the emission quenching and recovery is observed immediately following the addition of Co^{2+} or EDTA, respectively.

Viscosity Measurements

Further clarification of the interactions between the Ru(II) complexes 1, 2 and 3 and DNA was carried out by viscosity measurements. The viscosity of a DNA solution is sensitive to the addition of organic drugs and metal complexes bound by intercalation [32] Optical and photophysical probes provide necessary, but not sufficient, clues to support a binding model. Hydrodynamic measurements that are sensitive to length change (i.e. viscosity and sedimentation) are regarded as the least ambiguous and the most critical tests of a binding model in solution in the absence of crystallographic data [33–35]. A classical intercalation model demands that the DNA helix must lengthen as base pairs are separated to accommodate the binding ligand, leading to the increase of DNA viscosity. In contrast, a partial and/or non-classical intercalation of ligand bends the

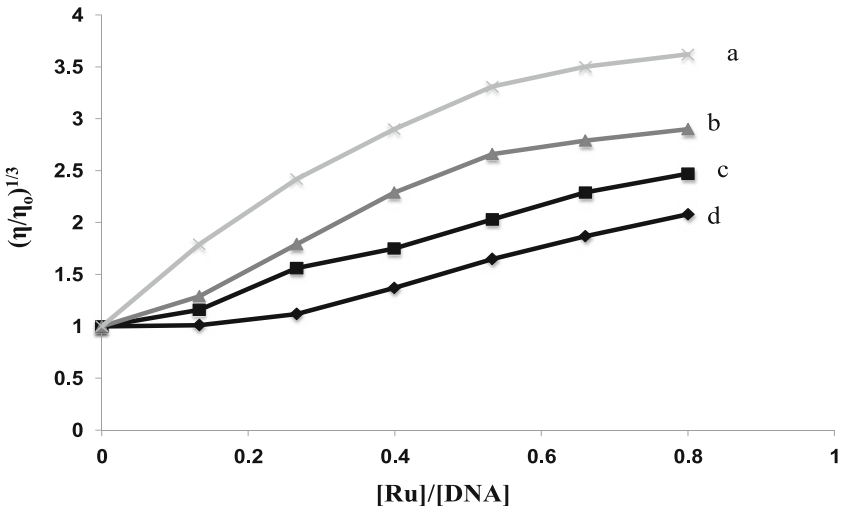

Fig. 8 Effect of increasing amounts of ethidium bromide (**a**), $[Ru(phen)_2(IPPBA)]$ (**b**),$[Ru(bpy)_2(IPPBA)]$ (**c**) & $[Ru(dmb)_2(IPPBA)]$ (**d**) on the relative viscosity of calf thymus DNA at 25(±0.1)°C. [DNA]=10 mM

Table 3 Results of DNA binding data of Ru(II) complexes

Complex	T_m	Hyopchromicity (%)	Absorption λ_{max}(nm) free bound	Δλ(nm)	K_b
$[Ru(phen)_2(IPPBA)]$	74	16.1	448–444	4	7.9×10^5
$[Ru(bpy)_2(IPPBA)]$	72	15.2	445–442	3	6.7×10^5
$[Ru(dmb)_2(IPPBA)]$	69	10.6	442–437	5	2.9×10^5

CT DNA T_M=60 °C

DNA helix, reduce its length and, concomitantly, its viscosity [19]. Viscosity of CT DNA (200 mM) has been measured in the presence of varying amount of complexes (20–140 mM). Effect of complexes **1**, **2** and **3** on the viscosity of rod like DNA is depicted in Fig. 8. On increasing the concentration of complexes **1**,**2** and **3** the relative viscosity of DNA increases steadily, which is similar to the behavior of classical intercalator like ethidium bromide and DPPZ . The results suggest that complexes **1**, **2** and **3** intercalate between the base pairs of CT DNA.

Melting Temperature

DNA melting is the process by which double-stranded DNA unwinds and separates into two unattached strands through the breaking of hydrogen bonding between the bases. The melting temperature (T_m) is defined as the temperature at which half of the DNA strands are in the double-helical state and half are in the "random-coil" state [36]. Thermal behaviors of DNA in presence of complex can give insight into their conformational changes when temperature is raised, and offer information about the interaction strength of complexes with DNA. The binding of metal complexes to the double-stranded DNA usually stabilizes the duplex structure to some extent depending on the mode and strength of their interaction with nucleic acid [37]. The melting curves of CT DNA in the absence and presence of $[Ru(phen)_2(IPPBA)](ClO_4)_2$, $[Ru(bpy)_2(IPPBA)](ClO_4)_2$ and $[Ru(dmb)_2(IPPBA)]$ $(ClO_4)_2$ are presented in (Table 3). The increase in the melting temperature values of Ru(II) complexes are comparable to the value observed with the classical intercalator etBr [38] and similar to those of DNA-intercalating Ru (II) polypyridyl complexes [39, 40]. It is clear from these figures that the complexes 1 and 2 are intercalators because the relative absorbance is high compared to that of the pure DNA sample. The increase in absorbance of the complexes follows the order 1>2>3.

Salt Independence

The binding of Ru(II) polypyridyl complexes to DNA is known to be highly sensitive to the presence of salt cations. This is due to the role played by electrostatic interactions in overall binding, which is reduced when salt cations interact with DNA phosphate groups. Moreover, the small size of these cations allows their insertion in DNA grooves and removes Ru(II) complexes from DNA(ruthenium(II) heteroleptic). According to the polyelectrolyte theory developed by Record et al., [41] the observed binding constant K is a function of the charge on the cation (Z), the fraction of counter ions associated with each DNA phosphate, and the concentration of Na^+. A plot of log K vs log $[Na^+]$ Fig. 9 is equal to SK in the following equation : $SK=(\delta \log[K_b]/\delta \log[Na^+])=-Z\psi$, where Z is the charge of the metal complex and ψ is 0.88 for double strand DNA. Figure 9 shows the decrease of K_b of complexes 1, 2 and 3 as the

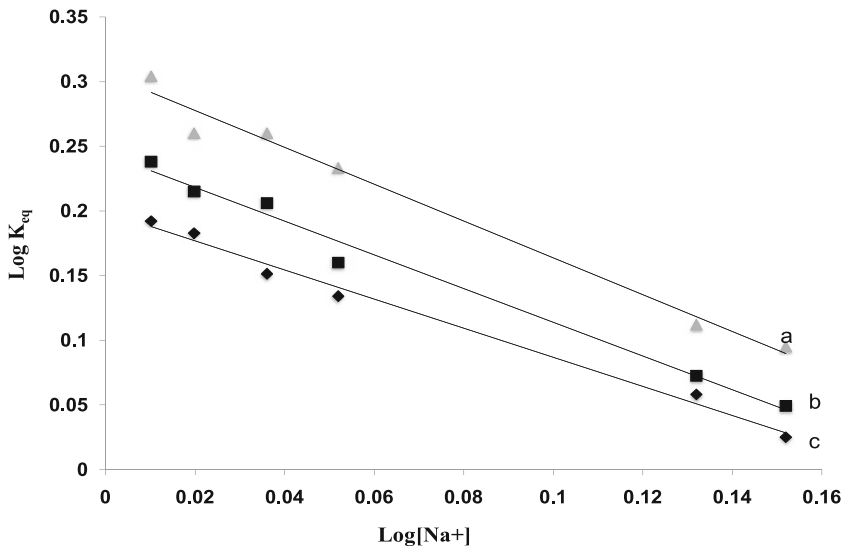

Fig. 9 Salt dependence of the equilibrium binding constants for DNA binding of complexes (**a**) $[Ru(phen)_2(IPPBA)]$, (**b**) $[Ru(bpy)_2(IPPBA)]$ & (**c**) $[Ru(dmb)_2(IPPBA)]$. The lines indicates the slope of the linear square fit to the data as (**a**) -1.96 (**b**) -1.82 (**c**) -1.42

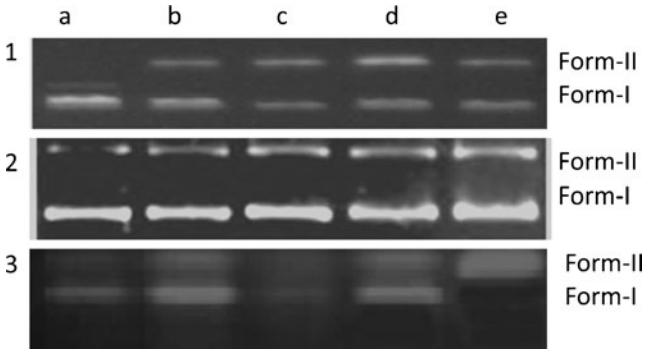

Fig. 10 Photocleavage studies of pBR322 DNA, in the absence and presence of complexes [Ru(phen)$_2$(IPPBA)] (1), [Ru(bpy)$_2$(IPPBA)] (2) and [Ru(dmb)$_2$(IPPBA)] (3) light after 30 min irradiation at 365 nm. Lane 0 control plasmid DNA (untreated pBR322), lane 1–6 addition of complexes in amounts of 10, 20, 30, 40, 50, 60 μL

concentration of Na^+ is increased [42]. As expected, the plot becomes nonlinear at ionic strengths greater than 0.1 M. [43–45]. The slopes of the lines in Fig. 9 are being −1.96, -1.82 and −1.42 for 1, 2 and 3 complexes respectively. The value of complex 1&2 are more than the theoretically expected values of Zψ (2×0.88=1.76) but complex 3 shows less value. Such lower values could arise from coupled anion release or from change in complex or DNA hydration upon binding. The knowledge of Zψ allows for a quantitative estimation of the non electrostatic contribution to the DNA binding constant for these complexes.

Photoactivated Cleavage of pBR 322 DNA by Ru(II) Complex

The irradiation of pBR322 plasmid DNA in the presence of the complexes was studied so as to determine the efficiency with which it sensitizes DNA cleavage. This can be achieved by monitoring the transition from the naturally occurring, covalently closed circular form (Form I) to the open circular relaxed form (Form II). This occurs when one of the strands of the plasmid is nicked, and can be determined by gel electrophoresis of the plasmid. Extended irradiation results in a build up of nicks on both strands of the plasmid, which eventually results in its opening to the linear form (Form III). When circular plasmid DNA is subjected to gel electrophoresis, relatively fast migration will be observed for the supercoiled form (Form I). Form (II) will migrate slowly and Form III will migrate between Form II and Form I [14, 46–49]. Figure 10 shows gel electrophoresis separation of pBR322 DNA after incubation with the complexes 1, 2 and 3 and irradiation at 365 nm. No DNA cleavage was observed for controls in which the complex was absent (lane 1). With increasing concentration of complexes 1, 2 and 3 Fig. 10 the amount of Form I of pBR 322 DNA diminish gradually, whereas Form II increases. At the concentration of 80 mM, complexes 1 and 2 can almost promote the complete conversion of DNA from Form I to Form II.

Table 4 Antibacterial activity of Ru(II) complexes

Complex	Bacterial species E.Coli	S. aureus
DMSO	Nil	Nil
$[Ru(phen)_2IPPBA]^{2+}$	19	12
$[Ru(bpy)_2IPPBA]^{2+}$	16	11
$[Ru(dmb)_2IPPBA]^{2+}$	13	15
Septomycine	20–22	12–14

Zone of inhibition of diameter in (mm)

Antibacterial Activities

Antitumor, anticancer and antimicrobial activity has been reported for some Ru(II) complexes substituted with imidazoles and Pyridines. The experimental results of the compounds were compared against DMSO as the control and are expressed as inhibition zone diameter (in mm) vs control Zone of inhibition was measured for three complexes as well as standard antibiotics and the results are given in (Table 4). The complexes 1 and 2 are very promising in exhibiting their ability to inhibit/destroy both Gram positive and Gram negative pathogenic bacteria. Complexation reduces the polarity of the metal ion because of the partial sharing of its positive charge with the donor groups. Chelation makes the chelating ligand more potent bactereostatic agents thus inhibiting the growth of bacteria more than the chelating ligands. Such complexation could enhance the lipophilic character of the central metal ion, which subsequently favours permeation through the lipid layers of cell membrane [50]. The antimicrobial activity of three complexes is in the order of 1>2>3.

Cytotoxicity

Cytotoxicity is a common limitation in terms of the introduction of new compounds into the pharmaceutical industry. In order to understand the in vitro cytotoxicities of the complexes 1, 2 and 3, experiments were carried out using four human tumor cell lines, like human cervical cancer (HeLa), Human breast adenocarcinoma cell line (MDA-MB-231 MCF-7) and (Human alveolar adenocarcinoma (A549). Complexes 1, 2 and 3 were dissolved in DMSO and blank samples containing same

Table 5 Percentage cell viability of different cell lines with ruthenium complexes

Complex	A549	MCF-7	HELA	MDA-MB-231
$[Ru(phen)_2IPPBA]^{2+}$(**1**)	0.798	2.582	18.185	7.952
$[Ru(bpy)_2IPPBA]^{2+}$ (**2**)	5.312	5.678	39.845	18.192
$[Ru(dmb)_2IPPBA]^{2+}$ (**3**)	28.29114	20.8069	30.517	25.973
Doxorubicin	1.21	1.05	0.451	0.501

Table 6 The H –Bond Vander Waals interactions and scores for binding of Ru(II) complexes to (2L8I) DNA containing CG bases using docking calculations

Complex	H –Bond donor- acceptor	Bond length (Å)	Vander Waals interactions (Complex – DNA)	Bond length (Å)	E (kcal/mol)
$[Ru(phen)_2(IPPBA)]^{2+}$	O51-DC25:HO3	1.723	C16-DC25:O3	2.579	50.423
	O51-DG24:H21	1.855	C54-DC25:O3	2.173	
	H79-DG24: N2	2.647	C10-DG4:H3	1.715	
	H80-DC25: O4	2.036	H59-DG4:H4	1.418	
$[Ru(bpy)_2(IPPBA)]^{2+}$	O50-DG1: H22	2.660	O50-DC25:O2	2.484	64.7574
	H79-DG1: N2	2.729	C22-DC5:OP1	2.558	
	H79-DC25: O2	1.482			
$[Ru(dmb)_2(IPPBA)]^{2+}$	H79-DG1: OP1	2.718	H75-DT3:H1	1.866	55.85
	O51-DC25: HO3	2.414	H75-DG24:H21	1.704	
			C40-DC25:HO3	2.004	
			H60-DC5:H5	1.773	
			C20-DG24:OP1	2.510	

volume of DMSO are taken as controls to identify the activity of solvent in this cytotoxicity experiment [51, 52]. The capabilities of complexes 1, 2 and 3 to arrest the proliferation of tumor cells without causing any damage to normal cells were evaluated after 48 h of incubation. The results were analyzed by means of cell viability curves and expressed as IC50 values. Table 5 displays the effect of complexes 1, 2 and 3 on cell growth at different concentrations. The biological assays of the metal complexes revealed that complex 1 exhibits enhanced activity against A549 cell lines when compared with complex 2 and 3 (IC50 0.798 mM) . On the other hand, complex 2 was found to be inactive against Hela cell lines in the dosage range 39 mM. Both the complexes 1 and 2 exhibited lesser in vitro cytotoxicity against tumor cell lines than Doxorubicin.

Docking Studies

To get further evidence for the binding model of metal complex with DNA, molecular docking studies were carried out. This is a computational procedure that attempts to predict non-covalent binding of a macromolecule (receptor) and a small molecule (ligand) efficiently. The goal is to predict the bound conformations and the binding affinity [21]. The prediction of the binding of small molecules to proteins/DNA is important because it is used to screen virtual libraries of drug-like molecules to obtain leads for further drug development. Docking can also be used to predict the bound conformation of known binders, when the experimental structures are unavailable. To obtain preliminary information regarding the structure of this synthesized complex and its interaction with DNA, docking was performed to find the most favorable orientation of the ligand/metal complex in DNA. Molecular docking studies have been successfully employed in rational drug design, but they have not been widely applied to study metal complexes. Although several docking programs, such as Gold, can tackle metal centers, it usually corresponds to part of a cofactor or an enzyme active site. Only a limited number of docking studies have been performed so far where the metal center is incorporated into the ligand being docked [23, 53].

In our experiment, molecular docking studies of complexes 1,2 and 3 with DNA duplex of sequence (GCTGCAAACGT CG/CGACGNTGCAGC) (PDB ID: 2L8I) were performed in order to predict the chosen binding site along with preferred orientation of the molecules inside the DNA groove (Table 6) show a preferential binding of complexes 1,2 and 3 between C-G base pairs, and bends the DNA slightly in such a way that a part of the molecule comes between the two base pairs of the DNA helix which makes favorable stacking interactions between the ring systems of the DNA bases and the IPPBA ring of complexes. In complex1, (Fig. 11) there are H-bonds between the OH groups of IPPBA and HO3/O4 of Cytosine at a distance of (1.723–2.036 Å) in addition to two bonds via N2/H21 of Guanine (2.647–1.855 Å) which conform minor groove interaction . The resulting binding energy of docked metal complexes 1, 2 and 3 were found to be −64.75, −55.85 and −50.423 Kcal/mol, respectively, correlating well with the

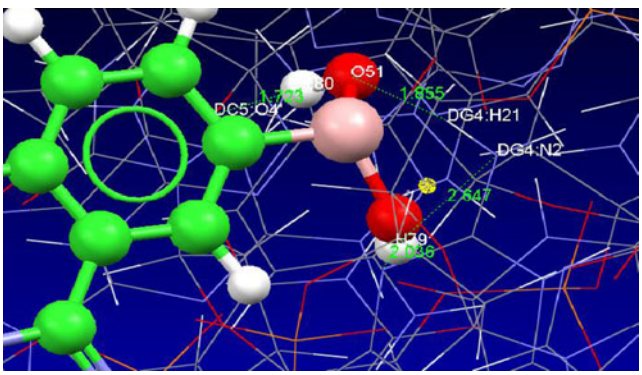

Fig. 11 Hydrogen bonds in DNA (PDB:2L8I) -docking models of complexes $[Ru(phen)_2(IPPBA)]$

experimental DNA binding values. The more negative the relative binding, the more potent the binding as between DNA and target molecules [54]. Thus, we can conclude that there is a mutual complement between spectroscopic techniques and molecular docked model, which can prove our spectroscopic results and at the same time provides further evidence of groove binding.

Conclusions

In summary, a new series of Ru(II) complexes have been synthesized and characterized. DNA-binding behaviors were investigated by absorption titration, viscosity measurements and thermal denaturation. The viscosity measurements show complexes 1 and 2 intercalate between the base pairs of DNA. Also, the complexes are efficient DNA-photocleavers upon irradiation at 365 nm, and complex 2 exhibits a stronger DNA-photocleavage efficiency than complex 1. In addition, in the presence of Co^{2+}, the emission of DNA-$[Ru(bpy)_2IPPBA]^{2+}$ can be quenched. The experimental results show that $[Ru(bpy)_2IPPBA]^{2+}$ exhibited the DNA "light switch" properties. The cytotoxicity assays suggest that complex 1 is more potent than complex 2. Groove binding of the DNA helix by Ru(II) complexes further validated by molecular docking studies.

Acknowledgements We are grateful to Indian Council for Cultural Relations (ICCR) Hyderabad for financial support and also CFRD Osmania University Hyderabad for helping the analysis and cytotoxicity studies.

References

1. Rosenberg B (1978) Platinum complexes for the treatment of cancer. Interdiscip Sci Rev 3:134–147
2. Kalyansundaram K (1992) Photochemistry of polypyridine and porphyrin complexes. Academic, London
3. Hannon MJ, Moreno V, Prieto MJ, Moldrheim E, Sletten E, Meistermann I, Isaac CJ, Sanders KJ, Rodger A (2001) Intramolecular DNA coiling mediated by a metallo supramolecular cylinder. Angew Chem Int Ed Engl 32:879–884
4. Friedman AE, Chambron JC, Sauvage JP, Turro NJ, Barton JK (1990) Molecular light switch for DNA: $Ru(bpy)_2(dppz)^{2+}$. J Am Chem Soc 112:4960
5. Shields TP, Barton JK (1995) Sequence-selective DNA recognition and photocleavage: a comparison of enantiomers of $Rh(en)_2phi^{3+}$. Biochemistry 34:15037
6. Shields TP, Barton JK (1995) A structural examination of enantioselective intercalation: ^1H NMR of $Rh(en)_2phi^{3+}$ isomers bound to $d(GTGCAC)_2$. Biochemistry 34:15049
7. Krotz AH, Kuo LY, Shields TP, Barton JK (1993) DNA recognition by Rhodium(III) polyamine intercalators: considerations of hydrogen bonding and van der waals interactions. J Am Chem Soc 115:3877
8. Sitlani AS, Long EC, Pyle AM, Barton JK (1992) DNA photocleavage by phenanthrenequinone diimine complexes of Rhodium(III): shape-selective recognition and reaction. J Am Chem Soc 114:2303
9. Barton JK, Raphael AL (1984) Photoactivated stereospecific cleavage of double-helical DNA by cobalt (III) complexes. J Am Chem Soc 106:2466
10. Pyle AM, Rehmann JP, Meshoyrer R, Kumar CV, Turro NJ, Barton JK (1989) Mixed ligand complexes of Ruthenium(II): factors governing binding to DNA. J Am Chem Soc 111:3053
11. Morgan RJ, Chatterjee S, Baker AD, Strekas TC (1991) Effects of ligand planarity and peripheral charge on intercalative binding of $Ru(2,2'\text{-bipyridine})_2$ L (2+) to calf thymus DNA. Inorg Chem 30:2687
12. Xiong Y, He XF, Zou XH, Wu JZ, Chen XM, Ji LN, Li RH, Zhou JY, Yu KB (1999) Interaction of polypyridyl ruthenium(II) complexes containing non-planar ligands with DNA. J Chem Soc, Dalton Trans 19–24
13. Sun D et al (2013) The effects of luminescent ruthenium(II) polypyridyl functionalized selenium nanoparticles on bFGF-induced angiogenesis and AKT/ERK signaling. Biomaterials 34(1):171–180
14. Kratochwil NA, Parkinson JA, Bednarski PJ, Salder PJ (1999) Nucleotide platination induced by Visible Light. Angew Chem Int Ed Engl 38:1460–1463
15. Marmur J (1961) A procedure for the isolation of DNA from microorganisms. J Mol Biol 3:208–218
16. Reichmann MF, Rice SA, Thomas CA, Doty P (1954) A further examination of the molecular weight and size of Desoxypentose Nucleic Acid. J Am Chem Soc 76:3047–3053
17. Yamada M, Tanaka Y, Yoshimoto Y, Kuroda Shimao S (1992) Synthesis and properties of diamino-substituted dipyrido [3, 2-a: 20, 30-c] phenazine. J Bull Chem Soc Jpn 65:1006–1011
18. Tan L-F, Chao H, Li H, Liu Y-J, Sun B, Wei W, Ji L-N (2005) Synthesis, characterization, DNA-binding and photocleavage studies of $[Ru(bpy)_2(PPIP)]^{2+}$ and $[Ru(phen)_2(PPIP)]^{2+}$. J inog Biochem 99:513–520
19. Sullivan BP, Salmon DJ, Mayer TJ (1978) Mixed Phosphine 2,2′-Bipyridine complexes of ruthenium. Inorg Chem 17:3334–3341
20. Satyanarayana S, Dabrowiak JC, Chaires JB (1993) Tris (phenanthroline) ruthenium (II) enantiomer interactions with DNA: mode and specificity of binding. Biochemistry 32:2573–2584
21. Liu JG, Ye BH, Li H, Zhen QX, Ji LN, Fu YH (1999) Polypyridyl ruthenium(II) complexes containing intramolecular hydrogen-bond ligand: syntheses, characterization, and DNA-binding properties. J Inorg Biochem 76:265–271
22. Mosmann T (1983) Rapid colorimetric assay for cellular growth and survival: application to proliferation and cytotoxicity assays. J Immunol Methods 65:55–63
23. Jones G, Willet P, Glen RC, Leach AR, Taylor R (1997) Development and validation of a genetic algorithm for flexible docking. J Mol Biol 267:727–748
24. Hoi-Ling S, Sze-Tin V, Kong-Wai T, Mohd Jamil M, Seik-Weng N, Raja Noor Zaliha Raja Abd R, Ignez C, Chew-Hee N (2010) Crystal structure, DNA binding studies, nucleolytic property and topoisomerase I inhibition of zinc complex with 1,10-phenanthroline and 3-methyl-picolinic acid. J Biometals 23:99–118
25. Jones G, Willet P, Glen RC (1995) Molecular recognition of receptor sites using a genetic algorithm with a description of desolvation. J Mol Biol 245:43–53
26. Gao F, Chao H, Zhou F, Yuan YX, Peng B, Ji LNJ (2006) DNA interactions of a functionalized ruthenium(II) mixed-polypyridyl complex $[Ru(bpy)_2ppd]^{2+}$. Inorg Biochem 100:1487–1494
27. Juris A, Balzani V, Barigelletti F, Campagna S, Belser P, Von Zelewsky A (1988) Ruthenium(II) polypyridine complexes: photophysics, photochemistry, electrochemistry, and chemiluminescence. Coord Chem Rev 84:85–277

28. Penumaka N, Naveena Latha J, Satyanarayana S (2006) DNA-binding studies of mixed-ligand (Ethylenediamine)ruthenium(II) complexes. Chemistry & biodiversity 3:1219
29. Chaires JB, Dattagupta N, Crothers DM (1982) Self association of daunomycin. Biochemistry 21:3927–3932
30. Joseph R, Lakowicz GW (1973) Quenching of fluorescence by oxygen. Probe for structural fluctuations in macromolecules. Biochemistry 12:4161–4170
31. Lakowicz JR (1983) Principles of fluorescence spectroscopy, Plenum Press York
32. Bai G, Dong B, Lu Y, Wang K, Jin L, Gao L (2004) A comparative study of the interaction of two structurally analogue ruthenium(II) complexes with DNA. J Inorg Biochem 98:2011–2015
33. Martell AE, Smith RM (1976) Critical stability constants. Plenum Press, New York
34. Deshpande MS, Kumbhar AA, Kumbhar AS, Kumbhakar M, Pal H, Sonawane UB, Joshi RR (2009) Ruthenium(II) complexes of bipyridine-glycoluril and their interactions with DNA. Bioconjugate Chem 20:447
35. Waring MJ (1965) Complex formation between ethidium bromide and nucleic acids. J Mol Biol 13:269–282
36. Neyhart GA, Grover N, Smith SR, Kalsbeck WA, Fairly TA, Cory M, Thorp HH (1993) Binding and kinetics studies of oxidation of DNA by oxoruthenium (IV). J Am Chem Soc 115:4423–4428
37. Shi S, Xie T, Yao TM, Wang CR, Geng XT, Yang DJ, Han LJ, Ji LN (2009) Synthesis, characterization, DNA-binding and DNA-photocleavage studies of $[Ru(bpy)_2(pmip)]^{2+}$ and $[Ru(phen)_2(pmip)]^{2+}$ (pmip = 2-(2′-pyrimidyl)imidazo[4,5-f] [1,10] phenanthroline. Polyhedron 28:1355–1361
38. Tselepi-Kalouli E, Katsaros N (1989) The interaction of $[Ru(NH_3)_5Cl]^{2+}$ and $[Ru(NH_3)_6]^{3+}$ ions with DNA. J Inorg Biochem 37:271–282
39. Barton JK (1986) Metals and DNA: molecular left-handed complements. Science 233–727
40. Vidhisha S, Kotha Laxma R, Ashwini Kumar K, Yata Praveen K, Satyanarayana S (2010) DNA interactions of ruthenium(II) complexes with a polypyridyl ligand: 2-(2, 5-dimethoxyphenyl)-1H-imidazo [4,5-f]1,10-phenanthroline. Transition Met Chem 35:1027–1034
41. Record MT Jr, Ha J-H, Fisher M (1991) Analysis of equilibrium and kinetic measurements to determine thermodynamic origins of stability and specificity and mechanism of formation of site-specific complexes between proteins and helical DNA. Methods Enzymol 208:291–343
42. Hargreaves VV, Schleif RF (2008) The salt dependence of the interferon regulatory factor 1 DNA binding domain binding to DNA reveals ions are localized around protein and DNA. Biochemistry 47:4119–4128
43. Sigma DS, Mazumder A, Perrin DM (1993) Chemical nucleases. Chem Rev 93:2295–2316
44. Shobha Devi C, Penumaka Nagababu M, Shilpa YP, Kumar MR, Reddy NM, Gabra SS (2012) Synthesis, characterization and DNA-binding characteristics of Ru(II) molecular light switch complexes. J Iran Chem Soc 9:671–680
45. Mynam Shilpa J, Naveena Latha A, Gayatri Devi A, Nagarjuna YP, Kumar PN, Satyanarayana S (2011) DNA–interactions of ruthenium(II) & cobalt(III) phenanthroline and bipyridine complexes with a planar aromatic ligand 2-(2-fluronyl)1H-imidazo[4,5-f][1,10-Phenanthroline]. J Incl Phenom Macrocycl Chem 70:187–195
46. Yata Praveen Kumar M, Shilpa P, Nagababu MR, Reddy KL, Reddy NM, Gabra SS (2011) Study of DNA light switch Ru(II) complexes : synthesis, characterization, photocleavage and antimicrobial activity. J Fluorescence 22:835–47
47. Basile LA, Barton JK (1987) Design of a double-stranded DNA cleaving agent with two polyamine metal-binding arms: Ru (DIP)2Macron. J Am Chem Soc 109:7548–7550
48. Gorver N, Guptha N, Singh P, Thorp H (1992) Studies of electrocatalytic DNA cleavage by oxoruthenium(IV). X-ray crystal structure of $[Ru(tpy)(tmen)OH_2](ClO_4)_2$ (tmen = N, N, N′, N′-tetramethylethylenediamine, tpy = 2, 2′, 2″ terpyridine). Inorg Chem 31:2014–2020
49. Kishikawa H, Jiang YP, Goodisman J, Dabrowiak JC (1991) Coupled kinetic analysis of cleavage of DNA by esperamicin and calicheamicin. J Am Chem Soc 113:5434–5440
50. Tweedy BG (1964) Possible mechanism for reduction of elemental sulfur by monilinia fructicola. Phytopathology 55:910
51. Xiong Y, Ji LN (1999) Synthesis, DNA-binding and DNA-mediated Luminescence Quenching of Ru(II) Polypyridine Complexes. J Coord Chem Rev 185–186:711–733
52. Liu JG, Zhang QL, Shi XF, Ji LN (2001) Interaction of $[Ru(dmp)_2(dppz)]_{2+}$ and $[Ru(dmb)_2(dppz)]^{2+}$ with DNA: effects of the ancillary ligands on the DNA-binding behaviors. Inorg Chem 40:5045–5050
53. Wolohan P, Reichert DE (2007) CoMSIA and docking study of rhenium based estrogen receptor ligand analogs. Steroids 72:247–260
54. Rocoux R, Bubuc R, Dupont C, Marechal JD, Martin A, Sellier M, Mahy JP (2008) Hemozymes peroxidases activity of artificial hemoproteins constructed from the Streptomyces liVidans xynalase A and irin(III)-carboxy substituted porphyrins. Bioconjugate Chem 19: 899–910